Astronomy & Astrophysics

LETTER TO THE EDITOR

Dust production scenarios in galaxies at $z \sim 6-8.3$

Aleksandra Leśniewska and Michał Jerzy Michałowski

Astronomical Observatory Institute, Faculty of Physics, Adam Mickiewicz University, ul. Słoneczna 36, 60-286 Poznań, Poland
e-mail: aleksandra.lesniewska@amu.edu.pl

ABSTRACT

Context. The mechanism of dust formation in galaxies at high redshift is still unknown. Asymptotic giant branch (AGB) stars and explosions of supernovae (SNe) are possible dust producers, and non-stellar processes may substantially contribute to dust production, for example grain growth in the interstellar medium.

Aims. Our aim is to determine the contribution to dust production of AGB stars and SNe in nine galaxies at $z \sim 6-8.3$, for which observations of dust have been recently attempted.

Methods. In order to determine the origin of the observed dust we have determined dust yields per AGB star and SN required to explain the total amounts of dust in these galaxies.

Results. We find that AGB stars were not able to produce the amounts of dust observed in the galaxies in our sample. In order to explain these dust masses, SNe would have to have maximum efficiency and not destroy the dust which they formed.

Conclusions. Therefore, the observed amounts of dust in the galaxies in the early universe were formed either by efficient supernovae or by a non-stellar mechanism, for instance the grain growth in the interstellar medium.

Key words. stars: AGB and post-AGB – supernovae: general – dust, extinction – galaxies: high-redshift – galaxies: ISM – quasars: general

1. Introduction

Dust in the Universe can absorb and re-emit up to 30% of starlight in the infrared (Hauser & Dwek 2001). Hence, the formation of dust has become one of the most important topics in galaxy evolution.

It is well known that there are two types of stellar sources that produce dust. Asymptotic giant branch (AGB) stars, which are evolved stars with initial masses of $0.8-8.0\,M_\odot$, create dust in their cooling dense ejecta. This process is associated with an intense phase of mass loss due to stellar winds, up to $10^{-4}\,M_\odot\,\mathrm{yr}^{-1}$ (Bowen & Willson 1991). They can dominate dust production as long as a burst of star formation took place at least 400 Myr prior to observations (Dwek et al. 2007; Valiante et al. 2009; Dwek & Cherchneff 2011). One AGB star is able to produce $10^{-5}-10^{-2}\,M_\odot$ of dust (Morgan & Edmunds 2003; Ferrarotti & Gail 2006; Ventura et al. 2012; Nanni et al. 2013, 2014; Schneider et al. 2014).

Supernovae (SNe) are another stellar source of dust. Dust formation takes place in the expanding ejecta a few hundred or thousand days after the explosion, and stellar progenitors have initial masses of $8-40\,M_\odot$.

Observations of SN1987A in the Large Magellanic Cloud have revealed that during such an event, up to $0.7\,M_\odot$ of dust could be created (Matsuura et al. 2011). Similarly, a large amount of dust, $\sim 0.5\,M_\odot$, has been reported for several supernovae (Gall et al. 2014; Owen & Barlow 2015; Bevan et al. 2017; De Looze et al. 2017; Temim et al. 2017; Rho et al. 2018; Chawner et al. 2019). This means that in the early galaxies a large amount of dust can be formed by SNe (e.g. Gall & Hjorth 2018). However, it is possible that SNe destroy

most of the dust they form by reverse shock waves (Temim et al. 2015; Bianchi & Schneider 2007; Cherchneff & Dwek 2010; Gall et al. 2011; Lakićević et al. 2015), but it is debated how much of the new and pre-existing dust is destroyed by a supernova as SN dust grains may be large and distributed in clumps (Gall et al. 2014; Lau et al. 2015; Wesson et al. 2015; Bevan & Barlow 2016; Micelotta et al. 2016; Gall & Hjorth 2018; Matsuura et al. 2019).

Dust grains formed by AGB stars and SNe can act as seeds that grow in the ISM, and this process can lead to a significant increase in the total dust mass (Draine & Salpeter 1979; Dwek & Scalo 1980; Dwek et al. 2007; Draine 2009). However, it is not clear if this process is efficient and quick enough, especially at high redshift. Ferrara et al. (2016) show that it is too slow in the diffuse ISM, and probably prohibited in molecular clouds because of icy mantles forming on the gas grains.

In this work we investigate a sample of galaxies at $6 < z < 8.4$ (900–600 Myr after the Big Bang) with the latest observational constraints on dust masses. Our aim is to test whether AGB stars or SNe are able to explain the observed amounts of dust in these galaxies, or whether dust accumulation must have also happened by a different (non-stellar) mechanism, for example grain growth in the ISM. We use a cosmological model with $H_0 = 70\,\mathrm{km\,s^{-1}\,Mpc^{-1}}$, $\Omega_\Lambda = 0.7$, and $\Omega_\mathrm{m} = 0.3$.

2. Sample

We have selected all galaxies at $z > 6$ for which observations of dust continuum have been attempted, except those for which a similar method has already been applied: quasars J1048+4637, J1148+5251, and J2054−0005 (Michałowski et al. 2010a), and

galaxies analysed in Michałowski (2015). We describe below the measurements used to estimate the dust and stellar masses needed for our analysis.

HATLAS J090045.4+004125 (hereafter HATLAS; Zavala et al. 2018) is one of a few submillimetre galaxies above $z = 6$ (together with that reported by Riechers et al. 2013). HATLAS was selected using the *Herschel* Space Observatory within the *Herschel* Astrophysical Terahertz Large Area Survey (Eales et al. 2010; Bourne et al. 2016; Valiante et al. 2016). Emission lines for ^{12}CO(6-5) and ^{12}CO(5-4) and the 1 mm continuum were detected by the Large Millimeter Telescope (Zavala et al. 2018). The mass of molecular gas was determined from the CO lines, whereas the dust mass was calculated in two ways: based on fitting photometric measurements to modified black-body function and via modelling using the MAGPHYS SED code (Table 1; Zavala et al. 2018). The dynamical mass was calculated using the isotropic virial estimator (Eq. 5 in Zavala et al. 2018).

Discovered with the Subaru telescope at redshift $z \sim 5.95$, HIMIKO was at that moment the most luminous Lyα emitter (Ouchi et al. 2009). Recent observations of this object using ALMA in band 6 revealed the presence of three clumps. From the [CII] detections the size of HIMIKO and the velocity linewidth were measured (Hirashita et al. 2017). The upper limit on the continuum emission of S158μm $< 27\,\mu$Jy was also reported. This is deeper than the previous ALMA data for this galaxy reported in Ouchi et al. (2013).

Cosmos Redshift 7 (CR7) located at $z = 6.6$ is the most luminous Lyα emitter, discovered using the Subaru Telescope (Matthee et al. 2015; Sobral et al. 2015). From the ALMA [CII] line detection and dust continuum upper limit, Matthee et al. (2017) estimated the dynamical masses and dust masses found in two regions of this galaxy, Clump A and Clump C-2 (Table 1).

SPT-S J031132−5823.4 (SPT0311−58) was discovered using the South Pole Telescope (Mocanu et al. 2013), and confirmed at a redshift of 6.9 (Strandet et al. 2017). With high-resolution ALMA observations, Marrone et al. (2018) detected continuum, [CII] 158 μm and [OIII] 88 μm lines of two components of SPT0311−58, named East and West, and determined their gas and dust masses. Only for SPT0311−58 East was the stellar mass determined because no stellar emission was detected for the West component.

SXDF-N1006-2 was discovered during a survey for Lyα Emitters (LAEs) by the Subaru Telescope (Shibuya et al. 2012) and is located at $z = 7.2$. Inoue et al. (2016) used ALMA to detect the [OIII] 88 μm emission line and, assuming that the galaxy is a circular disk, determined its dynamical mass (Table 1). The upper limit on the continuum flux at band 6 (1.33 mm) of <0.042 mJy was also obtained.

J1342+0928 is a quasar located at $z = 7.54$, first detected by Bañados et al. (2018). The detection of the [CII] 158 μm line emission allowed Venemans et al. (2017) to determine the dynamical mass of this galaxy based on the virial theorem, and the assumption that the [CII] emission comes from a rotating disk. From the detection of the 223.5 GHz continuum, the mass of dust in this galaxy was determined (Table 1). The limit on the molecular gas mass was derived from the observations of the CO(3-2) line (Table 1).

MACS0416_Y1 is one of the brightest Lyman Break Galaxies (LBGs) at $z \sim 8$ (Infante et al. 2015; Laporte et al. 2015). Using the detection of the [OIII] 88 μm line and the dust continuum, Tamura et al. (2019) confirmed its redshift as 8.3118, and measured its dust mass (assuming a dust temperature of 40 and 50 K). From the optical emission the stellar mass was determined

(Table 1). In our analysis, the lower error bar for the stellar mass was modified disregarding model solutions with ages lower than one million years (Tamura, priv. comm.).

A2744_YD4 at $z = 8.38$ is an LBG lensed by the Pandora Cluster. This object was observed in the *Hubble* Frontier Fields (HFF) by Zheng et al. (2014). The ALMA detection of the [OIII] 88 μm line allowed the confirmation of its redshift (Laporte et al. 2017). Based on the dust continuum detection and the optical emission, Laporte et al. (2017) estimated the mass of dust and stars in this galaxy (Table 1).

3. Method

We calculated the dynamical masses for galaxies with emission line detections for which this was not reported. This was the case for HIMIKO and SPT0311-58. Based on the detection of the [CII] emission line (Carniani et al. 2018; Marrone et al. 2018), the sizes of these galaxies were measured as $3.9 \pm 1.1 \times 1.7 \pm 1.1$ kpc for HIMIKO, 2.2 kpc for SPT0311-58E, and 7.5×2.0 kpc for SPT0311-58W. The [CII] linewidths were measured as 180 ± 50 km s^{-1} for HIMIKO, 500 km s^{-1} for SPT0311-58E, and 1000 km s^{-1} for SPT0311-58W. In order to calculate the dynamical masses we used Eq. (5) in Zavala et al. (2018), based on the isotropic virial estimator. The results of these calculations are flagged in Table 1 with dagger symbols (†).

Dust masses were not reported for HIMIKO and SXDF. We used the reported dust continuum upper limits to estimate the upper limits of the dust masses of these galaxies, assuming the dust temperature of 40 K and using Eq. (5) in Michałowski et al. (2009), based on Taylor et al. (2005) and Hildebrand (1983). A value of the emissivity index of $\beta = 2$ was assumed. This gives conservatively low dust masses (see Fig. 3 in Michałowski et al. 2010b). In particular, if we adopted $\beta = 1.5$, then we would obtain dust masses 2.7 times higher, which would make the stellar dust producers even less likely. If we used this method for all galaxies, not only for those whose dust masses have not been calculated elsewhere, we would obtain masses a factor of 0.84 ± 0.33 higher. This would not change any of our conclusions. The results of our adopted dust mass calculations are flagged in Table 1 with dagger symbols (†).

Using the same methodology as presented by Michałowski et al. (2010c) and Michałowski (2015), we determined the amount of dust that one star would have to produce in order to explain the observed amount of dust in every galaxy. The number of dust-producing stars was estimated from the stellar masses in the studied galaxies. The stellar masses were estimated in three ways: (1) as equal to $M_{\rm dyn}$ to obtain the maximum possible value, (2) as equal to $M_{\rm dyn} - M_{\rm gas}$, and (3) from SED modelling. The number of stars with masses between M_0 and M_1 can be calculated by the integration of the stellar initial mass function (IMF), according to the formula $N(M_0 - M_1) = M_{\rm stellar} \int_{M_0}^{M_1} \xi(M) {\rm d}M / \int_{M_{\rm min}}^{M_{\rm max}} \xi(M) M {\rm d}M$, where $\xi(M)$ is an IMF parametrised as $M^{-\alpha}$. We assumed $M_{\rm min} = 0.15$, $M_{\rm max} = 120\,M_\odot$, and three types of IMFs: the Salpeter (1955) IMF with $\alpha = 2.35$, the Kroupa (2001) IMF with $\alpha = 1.3$ in the mass range 0.15–0.5 $M_\odot$ and $\alpha = 2.3$ in the mass range 0.5–120 $M_\odot$, and a top-heavy IMF with $\alpha = 1.5$. The dust yield per star required to explain dust observed in a galaxy is then $M_{\rm dust}/N(M_0 - M_1)$.

At the redshifts of the studied galaxies the time since the Big Bang was short, such that low-mass stars had not had time to leave the main sequence and start producing dust during the AGB phase. Based on a lifetime on the main sequence of

Table 1. Physical properties of the galaxies in our sample.

	z	M_{dyn} $(10^{10}\,M_{\odot})$	M_{dust} $(10^{7}\,M_{\odot})$		M_{gas} $(10^{11}\,M_{\odot})$	M_{stellar} $(10^{9}\,M_{\odot})$		Ref.
HATLAS	6.027	2.6	19 ± 4	42 ± 7	0.16 ± 0.06	–		1
HIMIKO	6.595	$1.168^{(\dagger)}$	$<0.16^{(\dagger)}$		–	35^{+15}_{-26}		2, 3
CR7	6.604	–	–		–	20		4
CR7 Clump A	6.601	3.9 ± 1.7	<0.81		–	–		5
CR7 Clump C-2	6.598	2.4 ± 1.9	<0.81		–	–		5
SPT0311-58E	6.9	$7.7^{(\dagger)}$	40 ± 20		0.4 ± 0.2	35 ± 15		6
SPT0311-58W	6.9	$54.222^{(\dagger)}$	250 ± 160		2.7 ± 1.7	–		6
SXDF	7.2	5	$<0.29^{(\dagger)}$		–	$0.347^{+0.616}_{-0.166}$		7
J1342+0928	7.54	<15	<3.2	24.5 ± 18.5	<0.12	–		8
MACS0416_Y1	8.3118	–	0.36 ± 0.07	0.82 ± 0.16	–	$4.8^{+6.8}_{-1.8}$	$5.1^{+7.1}_{-4.9}$	9
A2744_YD4	8.38	–	$0.55^{+1.96}_{-0.17}$		–	$1.97^{+1.45}_{-0.66}$		10

References. $^{(\dagger)}$ indicates the value determined in this work. (1) Zavala et al. (2018); (2) Carniani et al. (2018); (3) Ouchi et al. (2009); (4) Sobral et al. (2015); (5) Matthee et al. (2017); (6) Marrone et al. (2018); (7) Inoue et al. (2016); (8) Venemans et al. (2017); (9) Tamura et al. (2019); (10) Laporte et al. (2017).

$10^{10} \times [M/M_{\odot}]^{-2.5}$ (Kippenhahn & Weigert 1990), we assumed that at $z < 7.0$ only stars with masses between 3 and 8 $M_{\odot}$ would have had time to enter the AGB phase, whereas at $z \geq 7.0$ the range of 3.5–8 $M_{\odot}$ was assumed. For SNe we assumed that their progenitors had masses in the range of 8–40 $M_{\odot}$.

4. Results and discussion

Figure 1 shows the dust yield per star required to explain the dust mass for a given galaxy, using all possible combinations of dust and stellar masses. Galaxies considered elsewhere (Michałowski et al. 2010a; Michałowski 2015) are shown as grey symbols. The top and bottom panels assume that the dust is produced by SNe and AGB stars, respectively. Some regions have been highlighted. In the top panel are shown the theoretical dust yield per SN without dust destruction ($<1.3\,M_{\odot}$; Todini & Ferrara 2001; Nozawa et al. 2003) and with ~90% dust destruction ($<0.1\,M_{\odot}$; Bianchi & Schneider 2007; Cherchneff & Dwek 2010; Gall et al. 2011; Lakićević et al. 2015). We note that it is difficult to constrain the fraction of newly formed dust destroyed by a reverse shock (Micelotta et al. 2016), so a weaker dust destruction is also possible. In the bottom panel the maximum theoretical dust yield per AGB star is shown ($0.04\,M_{\odot}$; Morgan & Edmunds 2003; Ferrarotti & Gail 2006; Ventura et al. 2012; Nanni et al. 2013, 2014; Schneider et al. 2014).

Depending on the data available, the stellar mass was obtained in various ways: as $M_{\mathrm{dyn}} - M_{\mathrm{gas}}$, as M_{dyn}, and from SED modelling. Only for one object, SPT0311-58E, was it possible to determine the required dust yield per star with the three different assumptions on stellar mass, and they do not differ from each other by more than their uncertainties. For this galaxy the required dust yield per SN is about 0.1–$1\,M_{\odot}$. This is close to the maximum dust yield predicted by simulations and to the highest observed values. Therefore, it is in principle possible that dust in this galaxy was formed by SNe, but that would require weak dust destruction and very efficient production. We cannot accept a similar conclusion for AGB stars. One AGB star would need to create between 0.1 and 1 $M_{\odot}$ of dust to explain the dust mass in SPT0311-58E, which is significantly higher than the allowed values.

The dust yield per SN required to explain dust in the HATLAS galaxy is close to $1\,M_{\odot}$, so if they are responsible for the bulk of the dust production, then they would need to be maximally efficient and not to destroy any dust. AGB stars cannot be responsible for the dust production in this galaxy because the required dust yield per star is more than 10 times higher than the theoretical value.

In the case of galaxies SPT0311-58W, J1342+0928, and A2744_YD4 it is possible that SNe are responsible for the observed dust. Some dust destruction, but not a significant amount, by SNe would be allowed in these cases as the derived dust yields are above $0.1\,M_{\odot}$. This is in line with the result of Gall & Hjorth (2018) that dust in distant galaxies (including A2744_YD4) was formed by SNe, which requires very little dust destruction. Again, the required dust yields per AGB star for these three galaxies are significantly above the theoretical limit, so AGB stars have not contributed substantially to the dust production in these galaxies.

For the remaining four galaxies in our sample the data are of insufficient quality to constrain the dust production mechanism. HIMIKO, CR7, and SXDF only have upper limits for the mass of dust, so we cannot rule out either SNe or AGB stars as dust producers. We can only conclude that one SN in these galaxies could not produce more than $0.01\,M_{\odot}$ of dust. This indicates that SNe in the early Universe are much less efficient than the maximum theoretical values, and casts doubts on the efficient SN dust production in the remaining galaxies in our sample (see also Hirashita et al. 2014). Our limit is two times deeper than that obtained by Hirashita et al. (2014) because we used stellar masses that are two times higher. For the last galaxy, MACS0416_Y1, we also cannot rule out the dust production mechanism because the large uncertainty on the measurement of its stellar mass results in a derived dust yield consistent with zero.

In summary, AGB stars were not able to form dust in the majority of $z > 6$ galaxies. Our results are conservative (leading to low required dust yields) because we include all stars that in principle could contribute to dust production. Stars with the masses close to our AGB lower limit (3 or 3.5 $M_{\odot}$) could have reached the AGB phase, but only if they were all born at the beginning of the galaxy evolution.
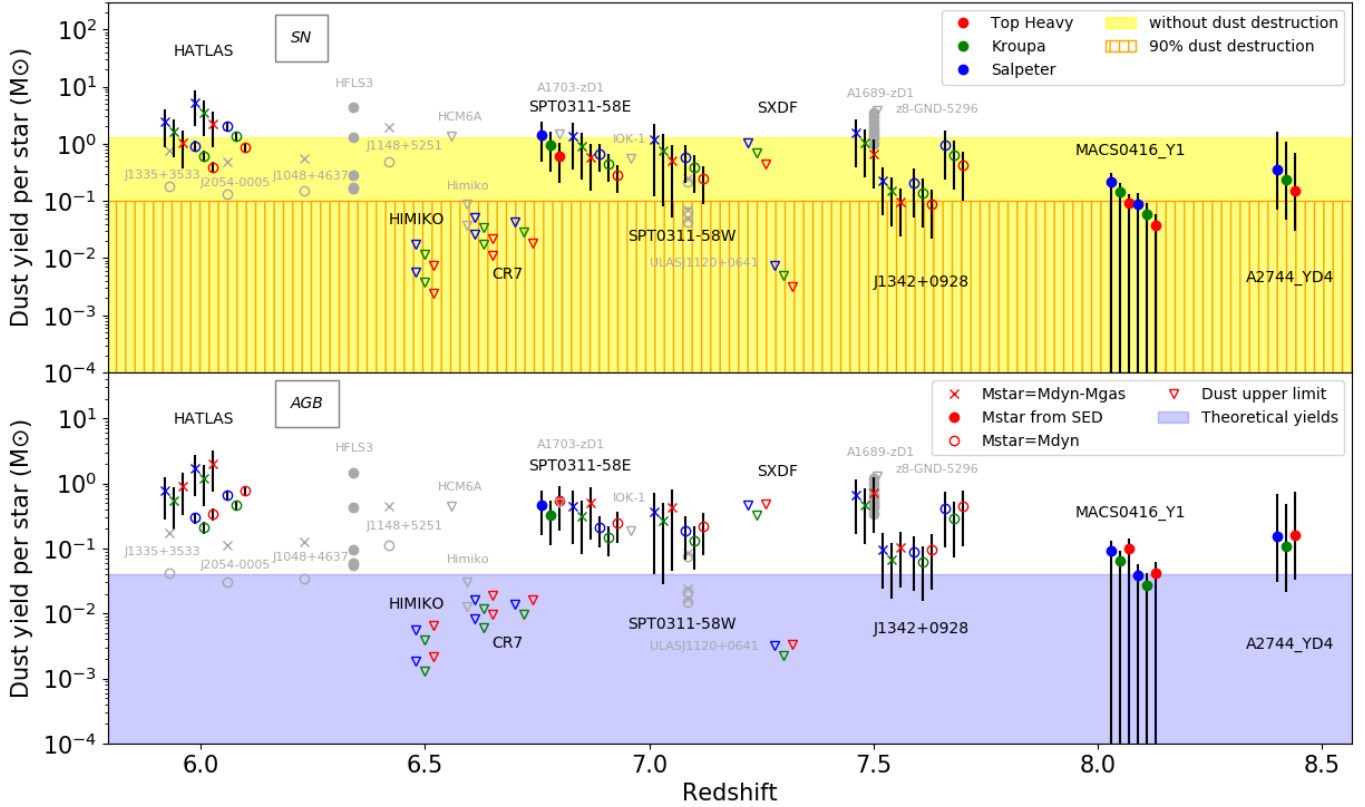
Fig. 1. Dust yield per SN (*top*) and AGB star (*bottom*) required to explain the dust masses in galaxies in our sample. Three forms of the initial mass function are assumed: top-heavy (red), Kroupa (green), and Salpeter (blue). The stellar mass was determined in various ways: $M_{dyn} - M_{gas}$ (cross), M_{dyn} (open circle), and SED modelling (filled circle). In addition, galaxies with upper limits of dust masses are indicated by down-pointing triangles. Multiple points with the same shape and colour for a galaxy are for different dust or stellar mass estimates. Galaxies considered elsewhere (Michałowski et al. 2010a; Michałowski 2015) are shown as grey symbols. For SNe two regions have been defined: below the maximum theoretical dust yield without dust destruction of 1.3 $M_\odot$ (yellow) and below the limit of 0.1 $M_\odot$ including ~90% dust destruction (vertical orange stripes). For AGB stars the theoretically allowed dust yields are indicated (light blue).

Supernovae would need to be maximally efficient and not to destroy the dust they formed (as in Hjorth et al. 2014; Gall & Hjorth 2018). One of the recent observations of SN 1987A indicates that dust can re-form and re-grow in post-shock region after being destroyed by the shock (Matsuura et al. 2019, but see Biscaro & Cherchneff 2014). This is consistent with high dust production efficiency of SNe. Similarly, the detection of SN dust in a 10 000 year old SN remnant (Lau et al. 2015; Chawner et al. 2019) indicates that dust is not efficiently destroyed by SNe.

It is unclear, however, whether all SNe can produce close to 1 $M_\odot$ of dust. If this is not the case, then some non-stellar mechanism is required, for example grain growth in the ISM. Asano et al. (2013) found that dust mass accumulation is dominated by the grain growth in the ISM if the metallicity is higher than a threshold value of 0.3 solar metallicity (or less if the star formation timescale is longer). This is likely for very dusty galaxies in our sample (HATLAS, SPT0311-58, J1342+0928), but more normal galaxies (MACS0416_Y1, A2744_YD4) may have lower metallicities. However, for A2744_YD4 we derived very high required dust yields per star, so either its metallicity is above this threshold or grain growth is always efficient below it.

We consider AGB stars and SNe separately, but in reality both contribute to dust production at the same time. However, this does not affect our conclusions because for the detected galaxies the required dust yields for AGB stars are approximately ten times higher than the allowed value. This means that

AGB stars could produce at most 10% of the dust in these galaxies, and thus considering AGB stars and SNe at the same time would lead to revising down the required dust yield per SN by only 10%.

The question remains of the source of heavy elements building the dust grains in these galaxies. Theoretical work has shown that each SN can produce around 1 $M_\odot$ of heavy elements (Todini & Ferrara 2001; Nozawa et al. 2003; Bianchi & Schneider 2007; Cherchneff & Dwek 2009). This is close to the required dust yields per SN in our sample, so, as do Michałowski et al. (2010a), we conclude that SNe are efficient enough to produce heavy elements needed to build dust grains in these galaxies, even if they do not directly form most of the dust.

5. Conclusions

We determined the dust yield per AGB star and SN required to explain the observed amount of dust in galaxies at redshift $6 < z < 8.4$. We obtained very high required dust yields per AGB stars, so they were not able to produce the majority of the dust in these galaxies. In most cases we accepted the hypothesis about the formation of dust by SNe, but they would need to be maximally efficient and not to destroy much dust. This suggests either that supernovae were efficient in producing dust in these galaxies or that a non-stellar mechanism was responsible for a significant fraction of dust mass accumulation, for example grain growth in the ISM.

References

Asano, R. S., Takeuchi, T. T., Hirashita, H., & Inoue, A. K. 2013, Earth Planets and Space, 65, 213
Bañados, E., Venemans, B. P., Mazzucchelli, C., et al. 2018, Nature, 553, 473
Bevan, A., & Barlow, M. J. 2016, MNRAS, 456, 1269
Bevan, A., Barlow, M. J., & Milisavljevic, D. 2017, MNRAS, 465, 4044
Bianchi, S., & Schneider, R. 2007, MNRAS, 378, 973
Biscaro, C., & Cherchneff, I. 2014, A&A, 564, A25
Bourne, N., Dunne, L., Maddox, S. J., et al. 2016, MNRAS, 462, 1714
Bowen, G. H., & Willson, L. A. 1991, ApJ, 375, L53
Carniani, S., Maiolino, R., Smit, R., & Amorín, R. 2018, ApJ, 854, L7
Chawner, H., Marsh, K., Matsuura, M., et al. 2019, MNRAS, 483, 70
Cherchneff, I., & Dwek, E. 2009, ApJ, 703, 642
Cherchneff, I., & Dwek, E. 2010, ApJ, 713, 1
De Looze, I., Barlow, M. J., Swinyard, B. M., et al. 2017, MNRAS, 465, 3309
Draine, B. T. 2009, in Cosmic Dust – Near and Far, eds. T. Henning, E. Grün, & J. Steinacker, ASP Conf. Ser., 414, 453
Draine, B. T., & Salpeter, E. E. 1979, ApJ, 231, 438
Dwek, E., & Cherchneff, I. 2011, ApJ, 727, 63
Dwek, E., & Scalo, J. M. 1980, ApJ, 239, 193
Dwek, E., Galliano, F., & Jones, A. P. 2007, ApJ, 662, 927
Eales, S., Dunne, L., Clements, D., et al. 2010, PASP, 122, 499
Ferrara, A., Viti, S., & Ceccarelli, C. 2016, MNRAS, 463, L112
Ferrarotti, A. S., & Gail, H.-P. 2006, A&A, 447, 553
Gall, C., & Hjorth, J. 2018, ApJ, 868, 62
Gall, C., Hjorth, J., & Andersen, A. C. 2011, A&ARv, 19, 43
Gall, C., Hjorth, J., Watson, D., et al. 2014, Nature, 511, 326
Hauser, M. G., & Dwek, E. 2001, ARA&A, 39, 249
Hildebrand, R. H. 1983, QJRAS, 24, 267
Hirashita, H., Ferrara, A., Dayal, P., & Ouchi, M. 2014, MNRAS, 443, 1704
Hirashita, H., Burgarella, D., & Bouwens, R. J. 2017, MNRAS, 472, 4587
Hjorth, J., Gall, C., & Michałowski, M. J. 2014, ApJ, 782, L23
Infante, L., Zheng, W., Laporte, N., et al. 2015, ApJ, 815, 18
Inoue, A. K., Tamura, Y., Matsuo, H., et al. 2016, Science, 352, 1559

Kippenhahn, R., & Weigert, A. 1990, Stellar Structure and Evolution (Springer)
Kroupa, P. 2001, MNRAS, 322, 231
Lakićević, M., van Loon, J. T., Meixner, M., et al. 2015, ApJ, 799, 50
Laporte, N., Streblyanska, A., Kim, S., et al. 2015, A&A, 575, A92
Laporte, N., Ellis, R. S., Boone, F., et al. 2017, ApJ, 837, L21
Lau, R. M., Herter, T. L., Morris, M. R., Li, Z., & Adams, J. D. 2015, Science, 348, 413
Marrone, D. P., Spilker, J. S., Hayward, C. C., et al. 2018, Nature, 553, 51
Matsuura, M., Dwek, E., Meixner, M., et al. 2011, Science, 333, 1258
Matsuura, M., De Buizer, J. M., Arendt, R. G., et al. 2019, MNRAS, 482, 1715
Matthee, J., Sobral, D., Santos, S., et al. 2015, MNRAS, 451, 400
Matthee, J., Sobral, D., Boone, F., et al. 2017, ApJ, 851, 145
Micelotta, E. R., Dwek, E., & Slavin, J. D. 2016, A&A, 590, A65
Michałowski, M. J. 2015, A&A, 577, A80
Michałowski, M. J., Hjorth, J., Malesani, D., et al. 2009, ApJ, 693, 347
Michałowski, M. J., Murphy, E. J., Hjorth, J., et al. 2010a, A&A, 522, A15
Michałowski, M. J., Hjorth, J., & Watson, D. 2010b, A&A, 514, A67
Michałowski, M. J., Watson, D., & Hjorth, J. 2010c, ApJ, 712, 942
Mocanu, L. M., Crawford, T. M., Vieira, J. D., et al. 2013, ApJ, 779, 61
Morgan, H. L., & Edmunds, M. G. 2003, MNRAS, 343, 427
Nanni, A., Bressan, A., Marigo, P., & Girardi, L. 2013, MNRAS, 434, 2390
Nanni, A., Bressan, A., Marigo, P., & Girardi, L. 2014, MNRAS, 438, 2328
Nozawa, T., Kozasa, T., Umeda, H., Maeda, K., & Nomoto, K. 2003, ApJ, 598, 785
Ouchi, M., Ono, Y., Egami, E., et al. 2009, ApJ, 696, 1164
Ouchi, M., Ellis, R., Ono, Y., et al. 2013, ApJ, 778, 102
Owen, P. J., & Barlow, M. J. 2015, ApJ, 801, 141
Rho, J., Gomez, H. L., Boogert, A., et al. 2018, MNRAS, 479, 5101
Riechers, D. A., Bradford, C. M., Clements, D. L., et al. 2013, Nature, 496, 329
Salpeter, E. E. 1955, ApJ, 121, 161
Schneider, R., Valiante, R., Ventura, P., et al. 2014, MNRAS, 442, 1440
Shibuya, T., Kashikawa, N., Ota, K., et al. 2012, ApJ, 752, 114
Sobral, D., Matthee, J., Darvish, B., et al. 2015, ApJ, 808, 139
Strandet, M. L., Weiss, A., De Breuck, C., et al. 2017, ApJ, 842, L15
Tamura, Y., Mawatari, K., Hashimoto, T., et al. 2019, ApJ, 874, 27
Taylor, E. L., Mann, R. G., Efstathiou, A. N., et al. 2005, MNRAS, 361, 1352
Temim, T., Dwek, E., Tchernyshyov, K., et al. 2015, ApJ, 799, 158
Temim, T., Dwek, E., Arendt, R. G., et al. 2017, ApJ, 836, 129
Todini, P., & Ferrara, A. 2001, MNRAS, 325, 726
Valiante, R., Schneider, R., Bianchi, S., & Andersen, A. C. 2009, MNRAS, 397, 1661
Valiante, E., Smith, M. W. L., Eales, S., et al. 2016, MNRAS, 462, 3146
Venemans, B. P., Walter, F., Decarli, R., et al. 2017, ApJ, 851, L8
Ventura, P., di Criscienzo, M., Schneider, R., et al. 2012, MNRAS, 424, 2345
Wesson, R., Barlow, M. J., Matsuura, M., & Ercolano, B. 2015, MNRAS, 446, 2089
Wright, E. L. 2006, PASP, 118, 1711
Zavala, J. A., Montaña, A., Hughes, D. H., et al. 2018, Nat. Astron., 2, 56
Zheng, W., Shu, X., Moustakas, J., et al. 2014, ApJ, 795, 93